

Hybrid Polymer Solar Cells from Highly Reactive Diethylzinc: MDMO–PPV versus P3HT

Date J. D. Moet,[†] L. Jan Anton Koster,^{†,‡} Bert de Boer,[†] and Paul W. M. Blom^{*,†}

Zernike Institute for Advanced Materials, University of Groningen, Nijenborgh 4, NL-9747 AG Groningen, The Netherlands, and Dutch Polymer Institute, University of Groningen, Nijenborgh 4, NL-9747 AG Groningen, The Netherlands

Received February 28, 2007. Revised Manuscript Received July 24, 2007

The degradation of poly[2-methoxy-5-(3',7'-dimethyloctyloxy)-*p*-phenylene vinylene] (MDMO–PPV) during the processing of hybrid organic/inorganic bulk-heterojunction solar cells with zinc oxide (ZnO) from a molecular precursor as acceptor is reported. Upon addition of diethylzinc, the absorption spectrum of MDMO–PPV shifts to the blue, and hole transport through the polymer deteriorates dramatically, indicating a reduction of the conjugation length of the polymer backbone. To prevent polymer degradation through the breaking of trans vinyl bonds, regioregular poly(3-hexylthiophene) (P3HT) is introduced as the electron donor. This system of P3HT and precursor ZnO reveals an unchanged UV–vis absorption profile and zero-field hole mobility with respect to the pristine polymer as well as an improved photovoltaic performance with an estimated power conversion efficiency of 1.4% (AM1.5 global reference spectrum, 1 kW/m²).

Introduction

Polymer-based photovoltaic devices are an up-and-coming alternative to conventional, inorganic solar cells. These lightweight elements for solar energy conversion have various important advantages over their silicon counterparts, such as easy processing, mechanical flexibility, the potential for low-cost fabrication of large areas, and ample possibilities of optoelectronic tuning of their material properties. Today's most efficient polymer-based solar cells are constructed from an interpenetrating network of an electron-donating polymer and an electron-accepting material.¹ Intimate intermixing of the two components of such a bulk-heterojunction (BHJ) solar cell ensures efficient dissociation of strongly bound excitons that are generated upon illumination.² Subsequent charge transfer from the polymer to the n-type acceptor is followed by dissociation of the bound electron–hole pair and transport of the spatially separated holes and electrons through the respective phases to the electrodes.

Different classes of materials have been used as an electron acceptor in BHJ solar cells, such as fullerene derivatives,¹ n-type conjugated polymers,^{3,4} and inorganic semiconducting materials. The latter is perhaps the most versatile group:

mixtures of polymers with nanoparticles of TiO₂⁵ and ZnO,^{6–8} ZnO nanorods,⁹ CdSe nanorods¹⁰ and tetrapods,^{11,12} as well as polymers permeated in mesoporous networks of TiO₂^{13,14} have been successfully integrated in devices showing a photovoltaic effect. Another method of realizing a hybrid nanoscale heterojunction consists in adding to the polymer solution a molecular precursor that, via hydrolysis and condensation reactions, converts to the desired n-type metal oxide, e.g., TiO₂,^{15,16} in situ during spin-coating. This approach surmounts the common problem with the application of nanoparticles, which requires a common solvent for the polymer and the inorganic acceptor. Furthermore, as with polymer/nanoparticle systems, the high electron mobility of the inorganic phase can be utilized in favor of the photoinduced current.

Unfortunately, in polymer:TiO₂ solar cells from a molecular precursor the ill-defined structure of the metal oxide

* Corresponding author. E-mail: p.w.m.blom@rug.nl.

[†] Zernike Institute for Advanced Materials.

[‡] Dutch Polymer Institute.

- (1) Yu, G.; Gao, J.; Hummelen, J. C.; Wudl, F.; Heeger, A. J. *Science* **1995**, *270*, 1789.
- (2) Coakley, K. M.; McGehee, M. D. *Chem. Mater.* **2004**, *16*, 4533.
- (3) Veenstra, S. C.; Verhees, W. J. H.; Kroon, J. M.; Koetse, M. M.; Sweelssen, J.; Bastiaansen, J. J. A. M.; Schoo, H. F. M.; Yang, X.; Alexeev, A.; Loos, J.; Schubert, U. S.; Wienk, M. M. *Chem. Mater.* **2004**, *16*, 2503.
- (4) Mandoc, M. M.; Veurman, W.; Koster, L. J. A.; Koetse, M. M.; Sweelssen, J.; de Boer, B.; Blom, P. W. M. *J. Appl. Phys.* **2007**, *101*, 104512.

- (5) Kwong, C. Y.; Djurišić, A. B.; Chui, P. C.; Cheng, K. W.; Chan, W. K. *Chem. Phys. Lett.* **2004**, *384*, 372.
- (6) Beek, W. J. E.; Wienk, M. M.; Janssen, R. A. J. *Adv. Mater.* **2004**, *16*, 1009.
- (7) Koster, L. J. A.; van Strien, W. J.; Beek, W. J. E.; Blom, P. W. M. *Adv. Funct. Mater.* **2007**, *17*, 1297.
- (8) Beek, W. J. E.; Wienk, M. M.; Janssen, R. A. J. *Adv. Funct. Mater.* **2006**, *16*, 1112.
- (9) Ravirajan, P.; Peiró, A. M.; Nazeeruddin, M. K.; Graetzel, M.; Bradley, D. D. C.; Durrant, J. R.; Nelson, J. J. *J. Phys. Chem. B* **2006**, *110*, 7635.
- (10) Huynh, W. U.; Dittmer, J. J.; Alivisatos, A. P. *Science* **2002**, *295*, 2425.
- (11) Sun, B.; Marx, E.; Greenham, N. C. *Nano Lett.* **2003**, *3*, 961.
- (12) Sun, B.; Snaith, H. J.; Dhoot, A. S.; Westenhoff, S.; Greenham, N. C. *J. Appl. Phys.* **2005**, *97*, 014914.
- (13) Coakley, K. M.; McGehee, M. D. *Appl. Phys. Lett.* **2003**, *83*, 3380.
- (14) Coakley, K. M.; Liu, Y.; McGehee, M. D.; Frindell, K. L.; Stucky, G. D. *Adv. Funct. Mater.* **2003**, *13*, 301.
- (15) van Hal, P. A.; Wienk, M. M.; Kroon, J. M.; Verhees, W. J. H.; Slooff, L. H.; van Gennip, W. J. H.; Jonkheijm, P.; Janssen, R. A. J. *Adv. Mater.* **2003**, *15*, 118.
- (16) Slooff, L. H.; Wienk, M. M.; Kroon, J. M. *Thin Solid Films* **2004**, *451–452*, 634.

phase actually limits the current and thus the overall performance. At room temperature the titanium(IV) isopropoxide precursor is converted in air into amorphous TiO_2 , whereas crystallization of the metal oxide would require incompatibly high temperatures, well above $350\text{ }^\circ\text{C}$.¹⁷ To overcome this limitation, Beek et al. have successfully made polymer:ZnO hybrid BHJ cells with diethylzinc as precursor. Since ZnO crystallizes already at room temperature, moderate annealing temperatures can be used that are compatible with the presence of the conjugated polymer in order to prepare a well-performing inorganic semiconductor phase. From external quantum efficiency (EQE) measurements, they estimated promising power conversion efficiencies of 1.1% (AM1.5G, 1 kW/m^2).¹⁸ A possible disadvantage of this approach is that the ZnO phase in this hybrid system is constructed in situ from highly reactive diethylzinc, which might lead to degradation of the polymer. The predominant degradation mechanism of conjugated polymers is photo-oxidation,^{19,20} which generally leads to a deterioration of the photoconductivity and thus device performance under illumination in the presence of oxygen.²¹ In poly(*p*-phenylene vinylene) (PPV) derivatives this degradation presumably results in a decrease of the conjugation length of the backbone. Because the trans vinyl ($-\text{C}=\text{C}-$) bonds are the most reactive moieties in the backbone, the chemical reaction that is deliberately induced during spin-coating may accelerate the degradation of the polymer. This effect can be avoided with the use of a more stable polymer. Polythiophene derivatives, for example, do not contain vinyl moieties and are more resistant to oxidation than are PPVs under identical circumstances.²²

In this paper, we address the limitation of hybrid solar cells from a mixture of a dialkoxy-substituted PPV with precursor ZnO due to partial degradation of the polymer during processing. This degradation is visualized with absorption spectroscopy and is shown to have a large undesirable effect on charge carrier transport. Furthermore, we present an improvement in terms of power conversion efficiency by mixing diethylzinc with a substituted polythiophene, which is not affected by the chemical reaction during processing.

Experimental Section

Poly[2-methoxy-5-(3',7'-dimethyloctyloxy)-*p*-phenylene vinylene] (MDMO-PPV, weight-average molecular weight $M_w \sim 3 \times 10^5$ g/mol, polydispersity index ~ 2.7 , synthesized via the sulfinyl route) was obtained from TNO and used as received. Regioregular poly(3-hexylthiophene) (RR-P3HT, electronic grade; 98.5% regioregular; Rieke Metals, Inc.) was dissolved in distilled toluene, dedoped with hydrazine at $60\text{ }^\circ\text{C}$, and precipitated in methanol. The fraction collected was Soxhlet extracted for at least 64 h with methanol, *n*-hexane, CH_2Cl_2 , and finally CHCl_3 . The chloroform fraction was

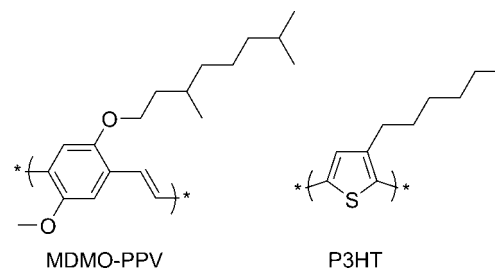


Figure 1. Chemical structures of the organic semiconductors used in this study. Left: poly[2-methoxy-5-(3',7'-dimethyloctyloxy)-*p*-phenylene vinylene] (MDMO-PPV); right: regioregular poly(3-hexylthiophene) (P3HT).

precipitated in methanol, dried under vacuum, and stored in the glovebox under a N_2 atmosphere. Properties of purified RR-P3HT: glass transition temperature $T_g \sim 130\text{ }^\circ\text{C}$, $M_w \sim 3 \times 10^5$ g/mol, polydispersity index ~ 2 . The structures of the polymers are shown in Figure 1.

The preparation procedure of a typical solar cell based on a bulk heterojunction of MDMO-PPV and precursor zinc oxide is described below. The fabrication of samples based on regioregular P3HT was done analogously.

A hole-transporting buffer layer of poly(3,4-ethylenedioxythiophene)/poly(styrene sulfonate) (PEDOT:PSS) was spin-coated on top of a UV ozone cleaned glass substrate, patterned with indium tin oxide (ITO). The photoactive layer was spin-coated from a mixed solution of MDMO-PPV and diethylzinc. This solution was prepared by the addition of the appropriate amount of a 0.4 M solution of diethylzinc in toluene and tetrahydrofuran (THF) to a solution of MDMO-PPV in chlorobenzene to give an overall polymer concentration of 5 mg/mL. Full conversion of diethylzinc into ZnO was assumed, which resulted in a volume fraction of 15 vol % ZnO in the heterojunction if a 1:1 weight ratio of the polymer and ZnO equivalent in the solution was used. The mixed solution (with a typical toluene to THF volume ratio of 1:2) was spin-coated in a nitrogen atmosphere with a relative humidity of $40 \pm 5\%$, controlled by the nitrogen flow through a gas diffusion bubbler. Subsequently, the hybrid film was aged for 15 min and annealed for 30 min at $110 \pm 5\text{ }^\circ\text{C}$ in the same environment. The back contacts, consisting of 1 nm lithium fluoride (LiF) or 5 nm samarium (Sm) topped with 100 nm aluminum (Al), were thermally deposited in vacuum ($\sim 10^{-6}$ mbar). So-called hole-only devices were constructed for hole transport studies by applying an electron blocking contact, consisting of 20–30 nm Pd and 60 nm Au, instead of the LiF/Al cathode. Together with an ITO/PEDOT:PSS bottom electrode, hole-ohmic contacts at both sides of the sandwiched layer were realized.

The current–voltage (J – V) characteristics were recorded with a Keithley 2400 SourceMeter in a nitrogen atmosphere, both in the dark and under illumination. The light source was a 50 W white light tungsten–halogen lamp. Because of the photocatalytic activity of ZnO (3.2 eV direct gap) that leads to the degradation of organic compounds in the UV region,²³ the lamp output was filtered with a Schott GG435 low-cut filter. The lamp/filter combination had a spectral range from 425 to 900 nm, with the maximum at 630 nm. The light intensity at the sample surface, i.e., after the UV filter, was $\sim 0.8\text{ kW/m}^2$ for MDMO-PPV:ZnO cells. P3HT:ZnO solar cells were characterized at ECN, The Netherlands, using a tungsten–halogen setup with an intensity of 1 kW/m^2 . Transmittance and absorbance measurements on polymer solutions in quartz

(17) Okuya, M.; Nakade, K.; Kaneko, S. *Sol. Energy Mater. Sol. Cells* **2002**, *70*, 425.

(18) Beek, W. J. E.; Slooff, L. H.; Wienk, M. M.; Kroon, J. M.; Janssen, R. A. *J. Adv. Funct. Mater.* **2005**, *15*, 1703.

(19) Scurlock, R. D.; Wang, B.; Ogilby, P. R.; Sheats, J. R.; Clough, R. L. *J. Am. Chem. Soc.* **1995**, *117*, 10194.

(20) Gelinck, G. H.; Warman, J. M. *Chem. Phys. Lett.* **1997**, *277*, 361.

(21) Neugebauer, H.; Brabec, C.; Hummelen, J. C.; Sariciftci, N. S. *Sol. Energy Mater. Sol. Cells* **2000**, *61*, 35.

(22) Cumpston, B. H.; Jensen, K. F. *Synth. Met.* **1995**, *73*, 195.

(23) Hoffmann, M. R.; Martin, S. T.; Choi, W.; Bahnemann, D. W. *Chem. Rev.* **1995**, *95*, 69.

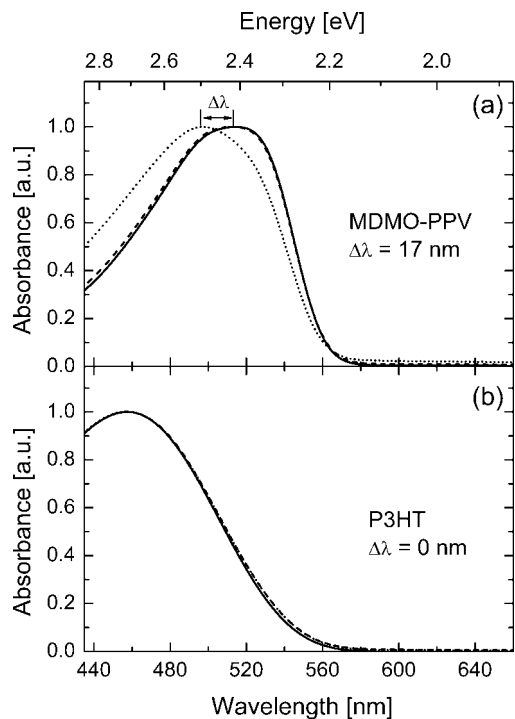


Figure 2. Absorption spectra of MDMO-PPV (a) and P3HT (b) in chlorobenzene, dissolved directly from the stock bottle (solid lines), redissolved from a processed layer of the neat polymer (dashed lines), and redissolved from a composite layer with precursor ZnO (dotted lines).

cuvettes were performed with a Perkin-Elmer Lambda 900 spectrometer.

Results and Discussion

The conversion of diethylzinc into ZnO is initiated upon exposure to water. Although the rate of the process is tempered by the addition of THF to the diethylzinc solution, it is important to keep the humidity of the surrounding atmosphere at a constant level. In spite of the high level of control of the relative humidity in our experiments, we measured large variations in the performance of MDMO-PPV:ZnO solar cells with 15 vol % ZnO and layer thicknesses of 100 ± 5 nm. Under illumination from a UV-filtered tungsten-halogen lamp with an intensity of ~ 0.8 sun, the most efficient cell gave a short-circuit current density J_{sc} of 20 A/m^2 , an open-circuit voltage V_{oc} of 1.03 V, and a fill factor FF of 41%. An identical device processed on another day, however, showed a substantially reduced performance: $J_{sc} = 8.3 \text{ A/m}^2$, $V_{oc} = 1.00 \text{ V}$, and $FF = 34\%$. The parameters of another 40 devices were scattered randomly between these two extremes, which resulted in a substantially lower average efficiency of $\sim 0.7\%$.

Because of this large variation in performance, an undesirable chemical side reaction is anticipated that has a detrimental effect on the structural and electronic properties of the polymer. In Figure 2a, the absorption spectrum of three different solutions of MDMO-PPV in chlorobenzene are shown. The solid line shows the absorbance of pristine MDMO-PPV dissolved directly after it was taken out of the stock bottle, whereas the dashed line represents the polymer after redissolving it from a pure MDMO-PPV layer that was spin-coated on top of a glass substrate and subsequently aged

and annealed in humid nitrogen. No effect on the absorption spectrum due to the processing under these conditions can be seen. However, a blue shift ($\Delta\lambda$) of 17 nm is found for the absorbance maximum of the polymer redissolved from a layer that was spin-coated from a mixture of MDMO-PPV and diethylzinc under humid conditions (dotted line). Such a blue shift is indicative of a reduction of the conjugation length of the polymer. Clearly, it is reasonable to expect that at least a small number of the most reactive moieties in the backbone of the polymer, i.e., the trans vinyl ($-\text{C}=\text{C}-$) bonds, are affected during the chemical process of precursor conversion. Moreover, the conversion of only a few percent of the vinyl double bonds to single bonds is known to strongly affect the transport of charge carriers through the polymer. Additionally, ^1H NMR measurements on a model compound that was mixed with diethylzinc and exposed to similar processing conditions indeed showed changes in the aromatic part of the NMR spectrum, attributed to disappearance of some of the vinyl bonds.²⁴ The most pronounced signs of degradation, however, were found in the deterioration of charge carrier transport.

The hole transport in light-emitting diodes based on MDMO-PPV is known to be space-charge limited.²⁵ This limitation arises from an accumulation of the low mobility charge carriers, which causes a redistribution of the electric field intensity that controls the charge transport properties in the bulk of the device. Characteristic for this space-charge-limited (SCL) regime is the square dependence on voltage (V) and inverse cubic dependence on thickness (L) of the current density (J). Recently, it has been demonstrated that at room temperature the dependence of the mobility on hole density is responsible for the increase of the SCL current at higher voltages.^{26,27}

Figure 3 shows the current densities under forward bias of hole-only devices from a neat MDMO-PPV layer (squares) and from a composite layer, in which ZnO is introduced via the conversion of diethylzinc (circles). Both layers were spin-coated, aged, and annealed in 40% relative humidity. The applied voltage was corrected for the built-in voltage (the voltage for which J becomes proportional to V^2) and the voltage drop over the series resistance of the ITO/PEDOT:PSS electrode (typically $25\text{--}40 \text{ }\Omega/\text{square}$) to obtain the internal voltage (V_{in}) over the active layer. The data of the MDMO-PPV device was fitted with a numerical

(24) Since ^1H NMR spectra of MDMO-PPV and P3HT result in broad and ill-defined resonance peaks, we mimicked the processing using the model compound (*E,E,E*)-1,4-bis[(4-styryl)styryl]-2-methoxy-5-(2'-ethylhexyloxy)benzene (MEH-OPV5), which was processed under similar conditions as the MDMO-PPV cells using diethylzinc. The pristine 5-ring oligomer MEH-OPV5 (*Polym. Prepr.* **2000**, *41*, 857) contains four olefinic vinyl moieties that are clearly resolved by ^1H NMR. When diethylzinc (in a toluene/THF mixture) is introduced during the processing procedure, new peaks appear between 7.84 and 7.69 ppm. Furthermore, several ill-defined multiplets arise between 3.53 and 2.41 ppm. These additional shifts are reconcilable with the formation of oxidized species such as alcohol or ketone and the complementary formation of saturated C-C bonds.

(25) Blom, P. W. M.; de Jong, M. J. M.; Vlegaar, J. J. M. *Appl. Phys. Lett.* **1996**, *68*, 3308.

(26) Tanase, C.; Blom, P. W. M.; de Leeuw, D. M. *Phys. Rev. B* **2004**, *70*, 193202.

(27) Tanase, C.; Meijer, E. J.; Blom, P. W. M.; de Leeuw, D. M. *Phys. Rev. Lett.* **2003**, *91*, 216601.

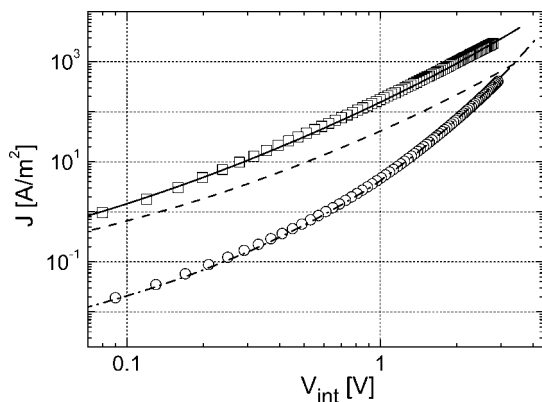


Figure 3. J - V characteristics of hole-only devices based on MDMO-PPV (\square) and MDMO-PPV:ZnO (\circ). The ITO electrode was positively biased. The solid line represents a numerical fit using the single carrier space-charge limited current with a density-dependent mobility. The dashed line shows the calculated J - V curve for the 95 nm thick MDMO-PPV:ZnO device, using the parameters from the fit of the pristine MDMO-PPV device ($L = 66$ nm). The dash-dotted line denotes a numerical simulation which takes into account a low mobility and a large field activation parameter.

device model,²⁸ using a density-dependent mobility (solid line). This resulted in a zero-field hole mobility $\mu_h(0) = 5 \times 10^{-10} \text{ m}^2/(\text{V s})$, a conductivity prefactor $\sigma_0 = 3.1 \times 10^7 \text{ S/m}$, an effective overlap parameter $\alpha^{-1} = 0.14 \text{ nm}$, and a width of the exponential density of states $T_0 = 518 \text{ K}$. Since these values are common for MDMO-PPV at room temperature, it is concluded that processing and annealing under humid conditions has no influence on hole transport in a pristine MDMO-PPV layer. Please note that the zero-field hole mobility of this batch of MDMO-PPV, which was synthesized via the sulfinyl route, is 10 times higher than previously reported for MDMO-PPV.^{25,26}

However, in a bulk heterojunction of MDMO-PPV and ZnO from diethylzinc (Figure 3, circles), the hole current density at lower voltages is about 2 orders of magnitude lower than in the pristine polymer layer and, moreover, the slope of J vs V is increased drastically. This can be seen more clearly by comparison of the measured data of this 95 nm thick hybrid device (circles) with its calculated J - V curve (dashed line). In the simulation, the above-mentioned parameters of the pristine MDMO-PPV layer were used, and only the layer thickness and dielectric constant were changed accordingly. The data of the hybrid layer could not be fitted with a purely density-dependent mobility because the strong bias dependence of J could not be recovered in the simulation. As an alternative indication of the deteriorated hole transport, the data have been fitted numerically using SCL currents with a high field activation parameter of the mobility and a low zero-field hole mobility (dash-dotted line in Figure 3). The resulting mobility of $1.8 \times 10^{-12} \text{ m}^2/(\text{V s})$ was more than 2 orders of magnitude lower than $\mu_h(0)$ in pristine MDMO-PPV, and the field activation parameter amounted to $1.32 \times 10^{-3} \text{ (m/V)}^{0.5}$. The latter value is abnormally high for a conjugated polymer, which makes justification of this interpretation difficult. It nevertheless confirms that processing

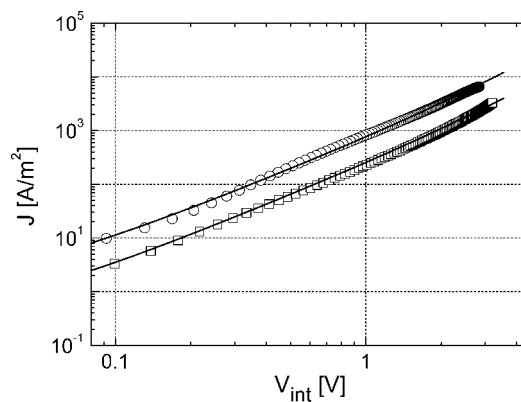


Figure 4. J - V characteristics of hole-only devices based on P3HT (\square) and P3HT:ZnO (\circ). The solid lines represent numerical fits using the single carrier space-charge-limited current with a density-dependent mobility. For both devices virtually the same parameters were used. The zero-field hole mobility amounted to $(2.2\text{--}2.5) \times 10^{-8} \text{ m}^2/(\text{V s})$.

MDMO-PPV together with diethylzinc in a humid environment has a huge undesired influence on the hole transport through the polymer.

We note that the incorporation of neutral traps for charge carriers in the polymer phase can also result in low currents and a high dependency on voltage. However, using the numerical device model with neutral traps that are exponentially distributed in energy, there was no combination of parameters that could simultaneously describe the temperature dependence of the hole current and its variation with sample thickness consistently. For a given set of parameters extracted from temperature dependence fits, the resulting calculated thickness scaling (see ref 29) of J was much stronger than the measured thickness dependence of the current density in multiple samples. Doubling the layer thickness resulted in a calculated current density that was an order of magnitude lower than the measured current; i.e., the dissimilarity was not caused by the uncertainty in the thickness measurements. Moreover, it was necessary to incorporate an additional field dependence of the mobility to obtain a good fit to the data. Therefore, trap-limited hole currents are inadequate in describing the observed effect.

The remarkable decay of hole transport possibly arises from field-assisted detrapping of holes in the polymer, in which charged traps might have been introduced due to interactions of diethylzinc with the polymer during processing of the layers. In this case, the escape rate of a hole from an oppositely charged trap is enhanced by the presence of an electric field, thus increasing the hole conductivity of the film.³⁰

The most important observation is that the transport properties of the polymer phase are strongly reduced by processing with diethylzinc. This contrasts with transport in MDMO-PPV:PCBM cells, in which the hole mobility is enhanced due to the presence of the acceptor phase,³¹ and with hole conduction in cells from MDMO-PPV and ZnO nanoparticles, in which no change in transport is found with respect to the pristine polymer.⁷ This effect thus forms a

(28) Koster, L. J. A.; Smits, E. C. P.; Mihailetchi, V. D.; Blom, P. W. M. *Phys. Rev. B* **2005**, *72*, 085205.

(29) Kao, K. C.; Hwang, W. *Electrical Transport in Solids*; Pergamon Press: Oxford, 1981.

(30) Frenkel, J. *Phys. Rev.* **1938**, *54*, 647.

(31) Melzer, C.; Koop, E. J.; Mihailetchi, V. D.; Blom, P. W. M. *Adv. Funct. Mater.* **2004**, *14*, 865.

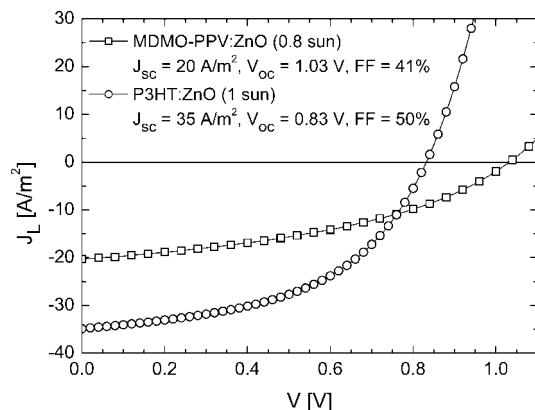


Figure 5. Comparison of the photovoltaic performance of ITO/PEDOT/MDMO-PPV:ZnO/LiF/Al (\square) and ITO/PEDOT/P3HT:ZnO/Sm/Al (\circ) solar cells with 15 vol % ZnO, made via the precursor route using diethylzinc.

major drawback in the use of MDMO-PPV for BHJ solar cells with precursor ZnO.

The changes in the hole current density in MDMO-PPV:ZnO devices are associated with the chemical reaction during processing. Obviously, using a chemically more stable conjugated polymer is the most direct way of avoiding the deterioration of hole transport due to degradation of the polymer during processing. By comparison of the absorbance, J - V characteristics, and fitted hole mobilities of P3HT with and without ZnO to the results on MDMO-PPV, we can conclude that P3HT is remarkably suitable for this purpose. Figure 2b clearly shows that the absorbance of P3HT in chlorobenzene is not influenced by first processing it under humid conditions, either in the presence of diethylzinc or without it. Also, as expected, the J - V curves of hole-only devices from P3HT and P3HT:ZnO layers had similar slopes (Figure 4). The fitted density-dependent hole mobility at room temperature as determined with numerical simulations was equal, within the experimental error, for P3HT:ZnO and neat P3HT layers that were spin-coated, aged, and annealed in nitrogen with 40% relative humidity. The fits resulted in $\mu_h(0) = (2.2\text{--}2.5) \times 10^{-8} \text{ m}^2/(\text{V s})$, $\sigma_0 = 1.6 \times 10^{-6} \text{ S/m}$, $\alpha^{-1} = 0.16 \text{ nm}$, and $T_0 = 425 \text{ K}$, being equal to earlier reported values for pristine P3HT layers.²⁷ This means that it is advantageous to use P3HT instead of MDMO-PPV in BHJ solar cells with precursor ZnO.

To obtain a one-to-one comparison, we prepared photovoltaic devices from P3HT:ZnO with 15 vol % ZnO using the same procedure as for cells from MDMO-PPV. The cells were characterized by incident-photon-to-current efficiency (IPCE) measurements and J - V measurements (at ECN, The Netherlands) under illumination from a UV-filtered tungsten-halogen lamp setup with an intensity of about 1 kW/m^2 . A cell with a layer thickness of 102 nm resulted in a J_{sc} of 35 A/m^2 , a V_{oc} of 0.83 V, and a FF of 50%. This is illustrated in Figure 5, together with the J - V curve of the most efficient MDMO-PPV:ZnO device of 96 nm thickness, measured at 0.8 sun intensity.

To account for the spectral mismatch, an estimation for J_{sc} of the P3HT:ZnO device under standardized AM1.5G, 1 kW/m^2 illumination ($J_{sc,calc}$) was made from the IPCE

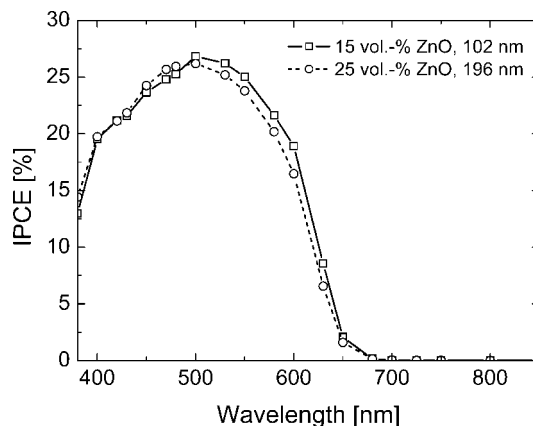


Figure 6. Incident-photon-to-current efficiency spectra of P3HT:ZnO solar cells with a ZnO content of 15 vol % (\square) and 25 vol % (\circ). The lines serve to guide the eye.

spectrum (see Figure 6, squares). This was done by calculation of the spectral response from the IPCE data and integration of its product with the AM1.5G spectrum over the wavelength range from 380 to 950 nm, after making sure that the short-circuit current was linearly dependent on light intensity. The resulting calculated short-circuit current density amounted to 33 A/m^2 , which is a factor of 1.4 higher than the $J_{sc,calc}$ previously reported for MDMO-PPV:ZnO cells.¹⁸ It was then used together with the V_{oc} and FF from the J - V measurements to obtain an estimated value of the AM1.5G power conversion efficiency (PCE) of 1.4%. To our knowledge, this is the highest PCE of a precursor route hybrid BHJ solar cell. Furthermore, a working system of P3HT and precursor ZnO has not been presented before.

The improvement of the photovoltaic performance is mainly due to the large increase in J_{sc} . Unfortunately, this positive effect is opposed by a decrease in V_{oc} of 0.2 V. This loss cannot be reduced, since the open-circuit voltage is a bulk property. For BHJ cells with ohmic contacts, V_{oc} is governed by the energy difference between the highest occupied molecular orbital (HOMO) of the donor and the lowest unoccupied molecular orbital (LUMO)³² or, in this case, the conduction band edge (CBE) of the acceptor. Because the HOMO level of regioregular P3HT ($\sim 4.9 \text{ eV}$) is several tenths of an electronvolt closer to the CBE of ZnO than is the HOMO level of MDMO-PPV ($\sim 5.2 \text{ eV}$), the observed reduction in V_{oc} is, most likely, inevitable.

To further explore the potential of P3HT for solar cells with precursor ZnO, we fabricated devices with a ZnO content of 25 vol % and layer thicknesses of about 200 nm. Assuming that the hole mobility in P3HT remains as high as before and that the percolation of the acceptor phase in the polymer matrix is enhanced by the increased amount of ZnO in the blend, one expects higher currents and thus an improved efficiency. Figure 6 demonstrates, however, that the IPCE spectra of the 25 vol % ZnO and 15 vol % ZnO cells have similar shapes and maxima of

(32) Mihailitchi, V. D.; Blom, P. W. M.; Hummelen, J. C.; Rispen, M. T. *J. Appl. Phys.* **2003**, *94*, 6849.

~26% at 500 nm. The calculation of the AM1.5G current for a 25 vol % ZnO cell gave a $J_{\text{sc,calc}}$ of 32 A/m², which, combined with a measured V_{oc} of 0.73 V and FF of 47%, resulted in an estimated AM1.5G PCE of 1.1%. This efficiency is somewhat lower than in the P3HT photovoltaic cells with 15 vol % ZnO. From additional J - V measurements on layers with thicknesses of up to 250 nm, however, we expect that the optimal thickness for the 25 vol % ZnO system is to be found beyond the 200 nm presented here. Further optimization of the hybrid polymer/ZnO system is needed in order to verify this.

In agreement with the results of Beek and co-workers,¹⁸ all precursor-route solar cells were found to withstand short-term UV illumination from a tungsten-halogen lamp without a significant decrease in performance. The shelf lifetime in nitrogen of unencapsulated P3HT:ZnO cells with 15 vol % ZnO was found to be limited due to a decrease of ~30% in both V_{oc} and FF under illumination from a halogen lamp after 46 h of storage, reducing the maximum power point to about half its initial value. A proportional reduction was found by comparison of the PCE as measured after 1 day in a solar simulator with a mismatch factor of 0.99 (measured at ECN, The Netherlands) to the calculated PCE as determined from the spectral response, which was measured shortly after processing. Strikingly, the short-circuit current was still at 80% of its original value after 1 week.

Conclusions

In conclusion, we have shown by means of UV-vis spectroscopy, ¹H NMR, and charge carrier transport studies that the presence of highly reactive diethylzinc during the processing of bulk heterojunctions of MDMO-PPV and ZnO causes the polymer to degrade. The degradation most likely involves a chemical reaction with trans vinyl bonds in the PPV backbone and the conversion to a nonconjugated species. Therefore, we have prepared photovoltaic devices of precursor ZnO and P3HT, which does not contain trans vinyl groups. No influence of the processing on the UV-vis absorption spectrum and hole transport properties of P3HT was found, indicating that diethylzinc does not affect this polymer. Without optimization, solar cells based on regio-regular P3HT and precursor ZnO had an estimated AM1.5G power conversion efficiency of 1.4% and hence currently belong to the best performing polymer/metal oxide photovoltaic devices.

Acknowledgment. The authors thank S. C. Veenstra and L. H. Slooff (ECN, The Netherlands) for IPCE and current-voltage measurements as well as discussions, T. C. Pijper and J. Wildeman (RuG, The Netherlands) for ¹H NMR measurements, and J. Harkema for technical assistance. The work of L. J. A. Koster forms part of the research program of the Dutch Polymer Institute (# 323).

CM070555U